EXPERIMENTAL INVESTIGATION OF FIRE RESISTANCE OF GLT BEAMS

L. KUCÍKOVÁ, T. JANDA, M. ŠEJNOHA & J. SÝKORA
Department of Mechanics, Czech Technical University in Prague, Czech Republic.

ABSTRACT
Mechanical and fire loading play together with geometric and material properties of glued laminated timber beams a decisive role in theoretical investigation into the time-dependent fire resistance of these elements. This is a multidisciplinary problem including heat conduction, water evaporation, internal gas pressure evolution, pyrolysis, volume change, etc. If properly calibrated, such complex models should allow us to forecast the evolution and shape of the charred or zero strength layer. It is doubtless that the calibration and validation steps require experiments. In particular, the results of large-scale fire experiment are discussed in this contribution focusing on the influence of fire intensity and duration on the temperature and the charred layer evolution. The influence of fire on stiffness and strength will also be addressed through the results of Pilodyn measurements of wood elastic modulus and three-point bending tests of original and fire-exposed beams.
Keywords: charred layer, fire curve, GLT beam, residual-bearing capacity.

1 INTRODUCTION

The wood is a natural material used, among others, as a fuel. As such it is combustible, which complicates its usage as a structural material. Therefore, a knowledge of its behavior during heating is crucial, especially at high temperatures. It is confirmed by many researchers that the wood mechanical properties are reduced with rising temperature, where the bending strength of spruce may decrease by about 50% after treatment at 220°C [1]. Kucíková *et al*. [2] reported a rapid decrease of modulus of rupture above 160°C and of modulus of elasticity (MOE) above 220°C. The safe temperatures are supposed to be below 65°C, where the influence of heat-treatment is negligible [3]. High temperatures also affect other properties, such as the density [4] and equilibrium moisture content, which is connected with the reduction of shrinkage and swelling [5]. The wood exposed to high temperatures also changes its color, which is referred to as browning [2]. These changes are caused by chemical processes that occur when heat is added to the system.

At temperatures rising above the 'safe temperature', the wood starts to lose water starting with the free water. The loss of bound water, i.e. the liquid water in the cell wall, follows next [1]. Further heat treatment causes decomposition of individual constituents (cellulose, hemicellulose, lignin, etc.) with a simultaneous formation of pyrolysis products (mainly volatile). Probably, the key process is the formation of char layer beginning at 300°C [6–7] or between 280°C and 300°C [8]. The most common approach to obtain residual capacity of wood members is based on the char layer formation related to 300°C isotherm. For more details regarding the processes at various temperatures, the reader is referred to [1, 6, 8].

The pyrolysis process is influenced by many aspects. First, it depends on the volume content of individual constituents and its structural composition. Also the moisture content plays a significant role, mainly in the initial stages of pyrolysis, where the water evaporation slows down the pyrolysis and results in a plateau occurring on a temperature curve at about 100°C [8]. The surrounding atmosphere naturally affects the rate of pyrolysis, where it is faster in the air containing oxygen in contrary to an inert atmosphere [5].

ISSN: 2046-0546 (paper format), ISSN: 2046-0554 (online), http://www.witpress.com/journals
DOI: 10.2495/CMEM-V8-N2-99-110

It is clear that developing a complex computational model to describe all processes taking place in wood during fire is rather challenging and calls for sufficient experimental data. Thus, describing our initiative experimental program represents the core of the present article whereas the potential approach to numerical simulations is outlined only briefly. The actual fire test is described in Section 2. The effect of height temperature on mechanical properties is examined in Section 3. The essential findings are finally provided in Section 5.

2 FIRE TEST

Fire tests are common methods of experimental investigation of structural members fire resistance. Among many apparatus used for these experiments, we have chosen a horizontal fire resistance test furnace as the most suitable for horizontal constructions.

Eight glued laminated timber (GLT) beams with cross section of 0.1 × 0.32 m and length of 2.38 m were tested. Each beam comprised eight lamellae attached together vertically, using melamine–urea–formaldehyde glue, and horizontally by finger joints. The lamellae were made of spruce wood cut from the parts near the tree center or even containing the pith (center). Each beam contained a certain amount of knots, cracks (mainly radial) and other imperfections. For illustration, one such a beam appears in Fig. 1 identifying dimensions of individual lamellae.

All beams were stored in the hall, where the fire test took place. Prior to test almost all samples were weighted and their dimensions were measured. Half of them were weighted after the fire test. All measured values are stored in Table 1. Photographs of individual beams were also taken to analyze the amount of knots, direction of growth rings and a number of performed using the Pilodyn 6J device, see Section 3, to acquire the elastic moduli of an

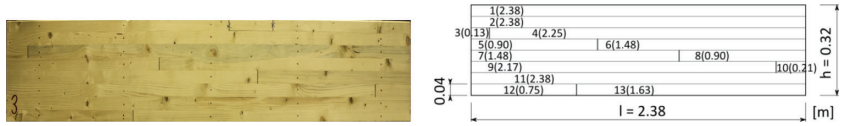

Figure 1: Example of GLT beam (width = 0.1 m).

Table 1: Weights and dimensions of beams measured before and after fire test.

Sample	Duration [min]	Weight (before) [Kg]	Weight (after) [Kg]	Length [m]	Height [m]	Width [m]
1	62	-	-	-	0.320	0.100
2	62	-	-	-	0.320	0.100
3	40	31.822	-	2.382	0.320	0.100
4	40	31.842	-	2.382	0.320	0.100
5	30	30.658	17.698	2.382	0.320	0.100
6	30	32.082	19.676	2.384	0.320	0.100
7	20	31.586	22.222	2.383	0.320	0.100
8	20	31.390	22.256	2.380	0.320	0.100

Table 2: Surface moisture content of beams measured before and after fire test.

Sample	MC (before) [%]	MC (after) [%]	MC (after - inside) [%]
3–4	-	5.44	-
5	10.54	-	-
6	11.05	9.22	-
7	11.17	9.61	-
8	10.70	8.81	14.41

intact timber. A capacitive hygrometer AHLBORN ALMEMO FHA 696 MF with an accuracy of 0.1% was used to examine the surface moisture content before and after the fire test, see Table 2 in which the value in the last column corresponds to the middle part of the cross section. Point out that the measurements denoted as 'after' took place almost immediately after extinguishing the fire by water stream.

2.1 Experimental set-up

The experimental set-up of the fire test was prepared in a way to simulate a real layout of the wooden ceiling. In each fire test, two GLT beams were placed on top of the furnace, isolated with the stone wool Isover UNI and finally covered with the oriented strand boards (OSB), see Figs. 2 and 3, to prevent heat escape from the furnace. This proved sufficient as the temperatures measured on the surface of OSB did not exceed 50°C for the longest fire duration.

In each experimental arrangement, one of the beams was equipped with 11 thermocouples placed in drilled holes with openings on the top of the beam. Every thermocouple represented different position within the cross section. Two types of thermocouple arrangement were considered. The top view scheme is plotted in Fig. 4, where the dashed line represents the middle of the beam. Thermal insulation boards were placed on the top of the beams to prevent damage caused by high temperatures. Unfortunately, during the first two experiments, the boards were lifted and the upper part of beams was burnt out, which partly affected the performance of several thermocouples. In the latter two tests, the holes with thermocouples were covered by ceramic blanket (Sibral), which prevented the upper part of the beams from being burnt.

Two settings of furnace temperature were used. The first one corresponded to the ČSN EN 1363-1 curve. The second one followed the beginning of the first curve, while at 600°C was

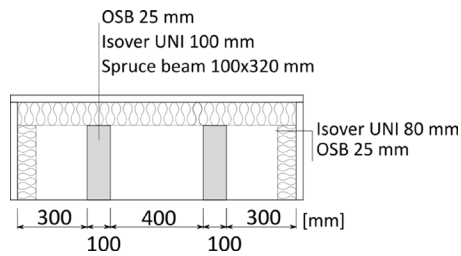

Figure 2: Experimental set-up for fire test.

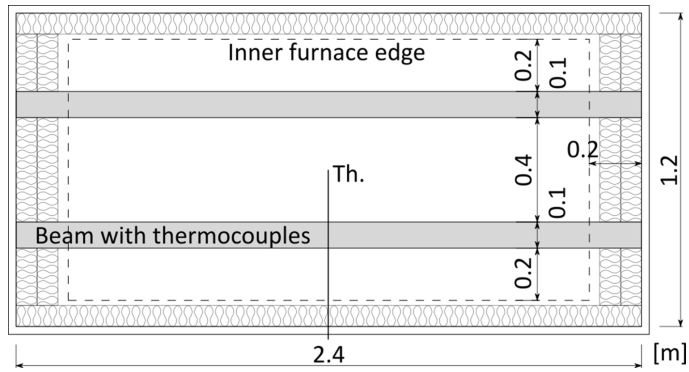

Figure 3: Scheme of the experimental set-up for fire test (Th. = thermocouple).

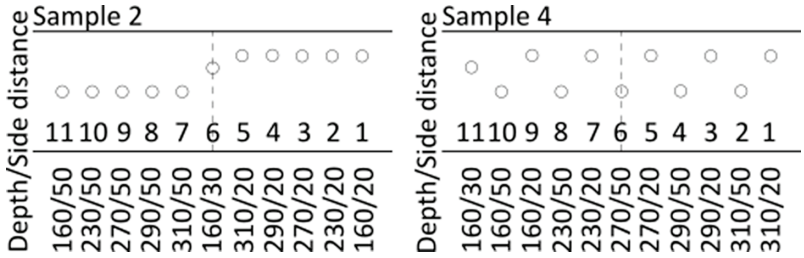

Figure 4: Arrangement of thermocouples—top view.

set constant. However, it is evident from the curves of actual temperature in the furnace depicted in Fig. 5 that the actual temperatures in the third and fourth experiment even exceeded the temperature in the previous tests. This is probably caused by the heat accumulation of the furnace construction. Unfortunately, in addition to temperature and time, it was not possible to measure other quantities. Ambient air was drawn into the furnace randomly, thus the inflow and oxygen concentration were not measured. Uncontrolled air ventilation (supply and exhaust) resulted in alternating both overpressure and underpressure in the furnace. A convective heat load was provided by gas burners placed on the bottom of a furnace chamber. The heat produced by burners was not measured.

During the experiment, the temperatures were simultaneously recorded using data loggers. The surface temperatures on OSB were controlled in 5 min steps and did not exceed 50°C. After required time (60 min, 40 min, 30 min and 20 min), the experiment was terminated. The burners were switched off, the thermocouples were cut off and the whole experimental arrangement was removed from the furnace. Subsequently, both beams were extinguished by water stream and taken out of the OSB box. This process took about 5–10 min. Finally, the beams were mechanically cleaned from charcoal layer and let to dry at ambient temperature.

2.2 Results

The loss of weight caused by fire showed a good correlation with the experiment duration. As seen in Table 1, the weight loss amounted to 9 kg and 12.5 kg for the test duration of 20 min

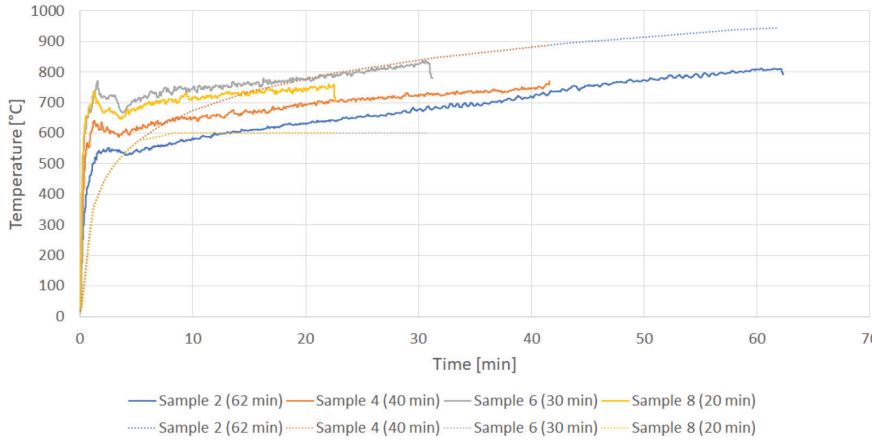

Figure 5: Actual (A) versus set (S) temperature curves.

and 30 min, respectively. Also the moisture content slightly decreased by about 2%, although this result could be affected by water used for fire extinguishing. The reduction of mechanical properties mentioned in the introductory section was also observed. Both measurements via indentation (Section 3.1) and three-point bending (Section 3.2) evinced decreased values.

Probably the main output of the fire test are temperature curves, describing the evolution of temperature with time. Wavy parts that indicated damage of thermocouples, mainly in the first two tests, or other inaccuracies were excluded. For illustration, we provide in Fig. 6, the evolution of temperature for the third experiment lasting 30 min.

As already mentioned in the introductory part, the plateaus observed for all curves in Fig. 6 at a temperature of about 100°C indicate water evaporation [8]. These are shorter for lower depths and are getting wider with increasing distance from the surface. Pozzobon *et al.* [9] confirmed this dependence experimentally, together with the dependence on the initial moisture content. Clearly, the onset of evaporation differs depending on the thermocouple position. At points closest to the bottom surface, these plateaus appeared within first 4 min of the experiment. In the middle part of the cross section, the evaporation temperature of 100°C has not even been reached.

Another important result is the amount of charred wood. This was evaluated from the cross-section images. To that end, the beams were cut in the transverse direction at nine

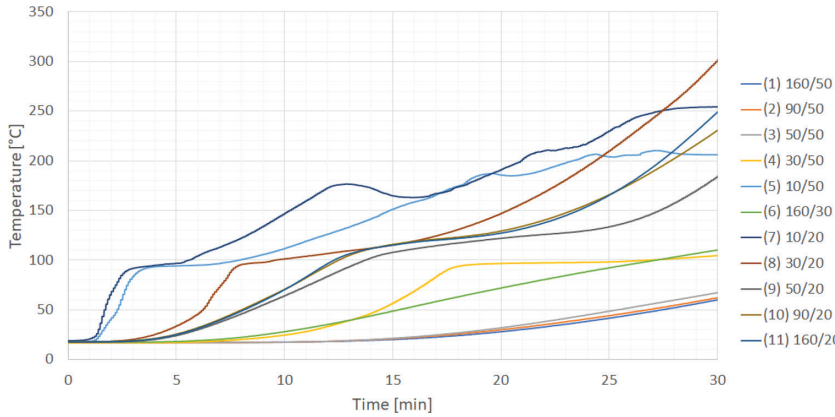

Figure 6: Temperature curves, sample 6, test duration 30 min.

locations along the beam being 0.25 m apart. Images of individual cross sections were scaled and inserted into the rectangle of 0.10 × 0.32 m representing the original cross section. The measurements were carried out on binary images, as shown in Fig. 7, where black and white color represents the residual cross section and the burnt part, respectively. The value of the residual cross section stored in Table 3 represents the remaining cross section after the fire test as a percentage of the original cross section. These cross sections show rounding of corners, which is a generally accepted phenomenon, also implemented in Eurocode 5 [11].

The charring depth, defined as 'the distance between the outer surface of the original member and the position of the char-line' according to EN 1995-1-2 [11] was also examined. Clearly, the charring depth measured from the bottom and top surfaces (i.e. along the vertical direction) is larger than in the horizontal direction, as stated by Thi *et al*. [12]. The thicknesses were measured at edges of four innermost lamellae, see Fig. 7e, where the boundaries of lamellae are depicted. The resulting values are summarized in Table 3.

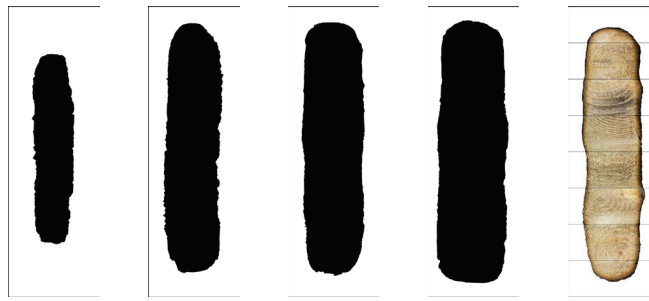

Figure 7: Residual cross sections taken from the center of the beam after fire test lasting: (a) 62 min, (b) 40 min, (c) and (e) 30 min and (d) 20 min.

Table 3: Results of image analysis performed on residual cross-sections.

Sample	Exp. duration [min]	Residual cross sec. [%]	Charring depth [mm]	Charring rate [mm/min]
1	62	27.01	31.21	0.50
2	62	27.43	29.47	0.48
3	40	45.41	21.61	0.54
4	40	46.93	20.50	0.51
5	30	52.26	18.60	0.62
6	30	56.21	18.89	0.63
7	20	63.22	14.52	0.73
8	20	64.02	14.30	0.71

The amount of burnt part and residual cross section, respectively, correlated well with the duration of fire test as evident from Fig. 7 and Table 3. The residual cross-section side edges are not straight but rather wavy. Seemingly, wider parts correspond to denser lamellae with thinner and more numerous growth rings. Knots, as the densest parts, protrude from the whole outline of the residual cross section as displayed in Fig. 7e.

The standard EN 1995-1-2 [11] provides a simple formula to calculate the design charring depth for standard fire exposure in the form

$$d_{char} = \beta t, \tag{1}$$

where d_{char} (mm) is the design charring depth, β (mm min^{-1}) the charring rate and t (min) the time of fire exposure. Considering this linear relationship allows us to estimate the mean charring rate by dividing the charring depth by the exposure time (duration of experiment). The results listed in the last column Table 3 are in accord with those provided by Štemberk [13]. The average charring rate, computed from the mean charring depth, decrease with the fire test duration. The same trend was also observed by Lange *et al*. [10], although the values were estimated from thermocouple measurements. This clearly indicates the time dependency of the instantaneous charring rate.

3 MECHANICAL TESTS

3.1 Indentation test

An indentation test using the Pilodyn 6J device was used in the present study to estimate the Young modulus of wood in the longitudinal direction [14]. In the present study, the Pilodyn was equipped with a spike of 2.5 mm in diameter and was driven into the wood in transverse direction with energy of 6 J to provide the value of penetration depth, d (mm) with an accuracy of 0.5 mm. The value of Young modulus then follows directly from an empirical equation written as

$$E = A + B\,d, \tag{2}$$

where constants A and B are determined experimentally. Herein, two sets of parameters were examined. The corresponding equations read

$$E_1 = 19.367 - 0.5641\,d\ (\mathrm{GPa}), \tag{3}$$

$$E_2 = 20.15 - 0.766\,d\ (\mathrm{GPa}). \tag{4}$$

Equation (3) is generally adopted when estimating the Young modulus of wood regardless of structural applications, whereas eqn (4) was proposed in [14] for particular application of GLT beams in bending.

The indentation measurements were performed on all samples before the fire test in the defined grid 5 × 8 points, located horizontally 0.2 m from the left side with 0.5 m gaps in between and vertically to the middle of each lamella. Altogether, there were 40 indents per beam in five vertical lines, so at least one indent was located in each lamella. Three beams, one for test durations of 20–40 min, were also tested after the fire test with larger number of points – 70 indents per beam. Their location was chosen randomly on both sides of the beam cleaned from charcoal.

The resulting mean values of Young's moduli together with the measured indentation depth are summarized in Table 4. While slight stiffness reduction is observed for all cases, no correlation with the fire test duration was identified. We expect to gain more relevant data from

Table 4: Pilodyn indentation.

	Pilodyn (before)			Pilodyn (after)		
Sample	**d [mm]**	**E_1[GPa]**	**E_2[GPa]**	**d [mm]**	**E_1[GPa]**	**E_2[GPa]**
1	13.08	11.99	10.13	-	-	-
2	12.81	12.14	10.34	-	-	-
3	13.20	11.92	10.04	-	-	-
4	14.03	11.46	9.41	17.57	9.45	6.69
5	13.85	11.55	9.54	-	-	-
6	13.18	11.93	10.06	19.36	8.44	5.53
7	13.43	11.79	9.87	-	-	-
8	14.16	11.38	9.30	19.01	8.64	5.59

standard tensile tests, where individual specimens can be linked to a particular temperature recorded during the fire test. This is because reliability of eqns (3) and (4) in application to wood exposed to elevated temperature is questionable as these were originally derived for wood without thermal degradation. The tensile tests are currently under way and the results will be presented elsewhere.

3.2 Three-point bending test

Three-point bending test belongs to common experiments for the determination of strength and bending MOE. This test was performed on four beams only; those free of thermocouples in the fire test.

Experimental set-up is depicted in Fig. 8a with a loading point in the middle of the beam. The beams were loaded in the displacement control regime with a loading rate of 0.02 mm s^{-1} until failure. Only the maximum displacement in the middle part of the beam was recorded, see Fig. 8b.

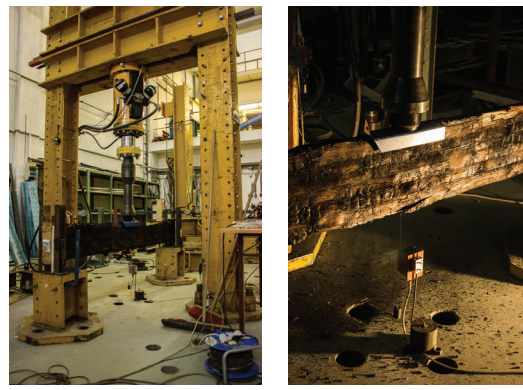

a) b)

Figure 8: Experimental set-up for three-point bending test.

Table 5: Three-point bending test.

Sample	Fire duration [min]	Load [kN]	Load time [min]
1	62	7.19	9.61
3	40	33.74	22.11
5	30	30.09	13.49
7	20	46.65	20.79

The resulting ultimate forces at the onset of essentially sudden failure are summarized in Table 5. As could be expected, the first beam, corresponding to the fire duration of 62 min, experienced the lowest bearing capacity; it withstood 7.19 kN only. On the other hand, the specimen with shortest fire load (duration of 20 min) was loaded up to 46.65 kN. Also notice that the load-bearing capacity of specimen No. 5 exposed to fire for 30 min (30.09 kN) did not exceed the load-bearing capacity of specimen No. 3 with fire duration of 40 min (33.74 kN). This could be attributed to a local defect or lower quality of wood in specimen No. 5.

4 NUMERICAL MODEL OF WOOD PYROLYSIS

The present section briefly outlines the numerical model we intend to adopt in the prediction of char layer formation during fire of GLT beams, so far examined in our study only experimentally. This is a multidisciplinary problem including heat conduction, pyrolysis mechanism, production of gas volatiles, volume change, water evaporation, internal gas pressure, properties of permeability and porosity and mechanical behavior. Some above-mentioned processes, such as thermal, physical and chemical ones, have already been coupled in a material modeling scheme commonly known as pyrolysis [15–16]. We refer the interested reader to an extensive review of the available material models reported by Shi *et al.* [17]. Almost all authors assume three fundamental processes which cannot be neglected in modeling of wood pyrolysis:

1. Pyrolysis reaction rate: Several different kinetic schemes were proposed to describe the conversion of the virgin fuel to gaseous products, tar and char. The two-step reaction scheme appears to be more complex pyrolysis mechanism, see Fig. 9. In this scheme, the virgin wood is decomposed during pyrolysis into the gas, char and tar, which is further simultaneously changed into the gas and char. All reactions are considered as irreversible and mathematically described by the Arrhenius law as

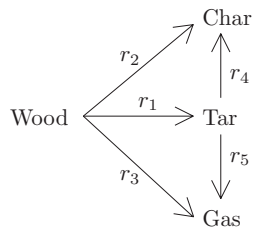

Figure 9: Pyrolysis two-steps reaction scheme.

Table 6: Kinetic data related to the two-step reaction scheme, see Fig. 9.

	$\mathbf{r_1}$	$\mathbf{r_2}$	$\mathbf{r_3}$	$\mathbf{r_4}$	$\mathbf{r_5}$
E_i[kJmol^{-1}]	112.7	106.5	88.6	108.0	108
A_i[s^{-1}]	$4.13 \cdot 10^6$	$7.38 \cdot 10^5$	$1.43 \cdot 10^4$	$1.00 \cdot 10^5$	$4.28 \cdot 10^6$

$$r_i = A_i \exp\left(\frac{-E_i}{R\theta}\right), \tag{5}$$

where A_i (s^{-1}) is the pre-exponential frequency factor, E_i (kJmol^{-1}) the activation energy, R (Jmol^{-1} K^{-1}) the universal gas constant and θ (K). Introducing such complex kinetic scheme places higher demands on the quality of input parameters, A_i and E_i. They are generally obtained from experimental measurements and typical kinetic data for two-step reaction scheme are summarized in Table 6.

2. Heat conduction: Thermal process plays a critical role in material models for wood pyrolysis. The heat transport inside the studied body is described by the conservation equation, which is in general form expressed as

$$\rho c_h \frac{\partial \theta}{\partial t} = \nabla \cdot (\lambda \nabla \theta) + \nabla \cdot \dot{m}_g \Delta h_g + Q. \tag{6}$$

This extended version of heat conduction equation was first introduced by Kung [18]. The first two terms represent the transient and spatial changes of temperature. Several studies, see e.g. [16], [17], have indicated that the accuracy of model prediction is enormously dependent on the correct description of thermal parameters. Therefore, it is inevitable to model the specific heat capacity and thermal conductivity as a function of temperature. The last terms stand for the convection heat of gas volatiles and heat loss/gain due to pyrolysis reactions.

3. Production of gas volatiles: Determination of individual gas volatiles, such as CO, CO_2 and H_2O, and their consequent transport is another important aspect of modeling the pyrolysis mechanism. According to [17], there are two main approaches predicting the production of gas volatiles. The first method is based purely on the experimental measurements and computes the gas volatiles directly as

$$\begin{aligned} \text{wood + required heat} \rightarrow 0.183\ \text{CO} + 0.115\ \text{CO}_2 + 0.047\ \text{CH}_4 + \\ 0.005\ \text{H}_2 + 0.25\ \text{H}_2\text{O} + 0.2\ \text{tar} + 0.2\ \text{char}. \end{aligned} \tag{7}$$

More complicated model is represented by the second approach. Here, the production rate of gas volatiles stems from the multi-steps reaction scheme utilizing average weight percentage of elements (C, H, O, N) contained in virgin wood.

5 SUMMARY AND CONCLUSIONS

An experimental program to address the influence of fire on residual mechanical properties of wood on the one hand, and to provide supporting data to model fire development under external heat flux in wood on the other hand, was executed. As expected, the results proved degradation of material properties with elevated temperatures and time-dependent rate of char layer formation. It also opened the way to examine the influence of fire from the

microstructure point of view. Evaluation of local properties, both geometrical and material, at the level cell wall from image analysis combined with nanoindentation is currently under way. Application of the numerical model briefly introduced in Section 4 will then benefit from the temperature curves acquired for several fire test durations. Validity of numerical prediction of char layer evolution will be tested against the images of residual cross-section.

ACKNOWLEDGEMENTS

The financial support provided by the GAČR grant No. 18-05791S is gratefully acknowledged.

REFERENCES

[1] Esteves, B.M. & Pereira, H.M., Wood modification by heat treatment: A review. *BioResources*, **4(1)**, pp. 370–404, 2009.

[2] Kačíková, D., Kačík, F., Čabalová, I. & Ďurkovič, J., Effects of thermal treatment on chemical, mechanical and colour traits in Norway spruce wood. *Bioresource Technology*, **144**, pp. 669–674, 2013. https://doi.org/10.1016/j.biortech.2013.06.110

[3] Winandy, J.E. & Rowell, R.M., Chemistry of wood strength. *Handbook of Wood Chemistry and Wood Composites*, ed. R.M. Rowell, CRC press: Boca Raton, Florida, pp. 303–347, 2005.

[4] Buchanan, A.H. & Abu, A.K., *Structural Design for Fire Safety*, 2nd ed. John Wiley & Sons Inc.: United Kingdom, 2017.

[5] Yildiz, S., Gezer, E.D. & Yildiz, U.C., Mechanical and chemical behavior of spruce wood modified by heat. *Building and Environment*, **41(12)**, pp. 1762–1766, 2006. https://doi.org/10.1016/j.buildenv.2005.07.017

[6] Dietenberger, M. & Hasburgh, L., Wood products thermal degradation and fire. *Reference Module in Materials Science and Materials Engineering*, pp. 1–8, 2016.

[7] Lineham, S.A., Thomson, D., Bartlett, A.I., Bisby, L.A. & Hadden, R.M., Structural response of fire-exposed cross-laminated timber beams under sustained loads. *Fire Safety Journal*, **85**, pp. 23–34, 2016. https://doi.org/10.1016/j.firesaf.2016.08.002

[8] Friquin, K.L., Material properties and external factors influencing the charring rate of solid wood and glue-laminated timber. *Fire and Materials*, **35(5)**, pp. 303–327, 2011. https://doi.org/10.1002/fam.1055

[9] Pozzobon, V., Salvador, S., Bézian, J.J., El-Hafi, M., Le Maoult, Y. & Flamant, G., Radiative pyrolysis of wet wood under intermediate heat flux: Experiments and modelling. *Fuel Processing Technology*, **128**, pp. 319–330, 2014. https://doi.org/10.1016/j.fuproc.2014.07.007

[10] Lange, D., Boström, L., Schmid, J. & Albrektsson, J., *The Influence of Parametric Fire Scenarios on Structural Timber Performance and Reliability*. Technical report, SP Technical Research Institute of Sweden, 2014.

[11] European Committee for Standardization, E.C., *Eurocode 5: Design of Timber Structures - Part 1-2: General -Structural Fire Design*, 2004.

[12] Thi, V.D., Khelifa, M., Oudjene, M., El Ganaoui, M. & Rogaume, Y., Finite element analysis of heat transfer through timber elements exposed to fire. *Engineering Structures*, **143**, pp. 11–21, 2017. https://doi.org/10.1016/j.engstruct.2017.04.014

[13] Štemberk, T., *Application of Wood in Modern Architecture*. Diploma thesis, University of West Bohemia, p. 129 (in Czech), 2018.

[14] Šejnoha, M., Janda, T., Melzerová, L., Nežerka, V. & Šejnoha, J., Modeling glulams in linear range with parameters updated using Bayesian inference. *Engineering Structures*, **138**, pp. 293–307, 2017. https://doi.org/10.1016/j.engstruct.2017.02.021

[15] Lautenberger, C. & Fernandez-Pello, C., Generalized pyrolysis model for combustible solids. *Fire Safety Journal*, **44(6)**, pp. 819–839, 2009. https://doi.org/10.1016/j.firesaf.2009.03.011

[16] Moghtaderi, B., The state-of-the-art in pyrolysis modelling of lignocellulosic solid fuels. *Fire and Materials*, **30(1)**, pp. 1–34, 2006. https://doi.org/10.1002/fam.891

[17] Shi, L. & Chew, M.Y.L., A review of fire processes modeling of combustible materials under external heat flux. *Fuel*, **106**, pp. 30–50, 2013. https://doi.org/10.1016/j.fuel.2012.12.057

[18] Kung, H.C., A mathematical model of wood pyrolysis. *Combustion and Flame*, **18(2)**, pp. 185–195, 1972. https://doi.org/10.1016/s0010-2180(72)80134-2